

## STRESS–STRAIN STATE OF SHALLOW SHELLS WITH RECTANGULAR PLANFORM AND VARYING THICKNESS: REFINED FORMULATION

A. Ya. Grigorenko and N. P. Yaremchenko

UDC 539.3

**The stress–strain state of a shallow shell with rectangular planform and varying thickness is analyzed in a refined formulation for different boundary conditions. A numerical-and-analytic method is developed based on the spline-approximation and discrete-orthogonalization methods. The stress–strain state of shallow shells with thickness varied without change in weight is analyzed**

**Keywords:** shallow shell, nonclassical model, spline-approximation, variable thickness

**Introduction.** Variable-thickness shells of various shapes are widely used in modern engineering structures of high strength and reliability. The fundamentals of the theory of shallow shells are outlined in [1, 4, 6, 7, 11, 12]. The strength analysis of such shells involves severe computational difficulties associated with the complexity of the original system of partial differential equations and the corresponding boundary conditions.

This paper analyzes the stress–strain state of shallow shells with rectangular planform and thickness varying in one or two coordinate directions. The shells are somehow fixed at their edges and are subjected to uniform normal pressure. The effect of variation in the thickness at constant weight on the strain–stress state of the shells is examined. The problem is solved in a nonclassical formulation based on a refined rectilinear-element model [2, 5, 17–19]. Note that the stress–strain state of shallow shells was studied numerically in [3, 8–10].

Recent trends in computational mathematics, mathematical physics, and mechanics are toward the wide use of spline functions to solve such problems. This is due to the following advantages of spline-approximations: (i) stability of splines against local perturbations (the local behavior of a spline at a point does not affect its overall behavior, unlike, for example, polynomial approximation); (ii) good convergence of spline-interpolation (unlike polynomial interpolation); and (iii) simplicity and convenience of numerical implementation of spline algorithms. When used in various variational, projective, and other discrete-continuous methods, spline functions yield much better results than classical polynomials do, simplify the numerical implementation of these methods, and improve the accuracy of the solution. The spline-collocation method proposed in [13–16] is developed here to analyze the stress–strain state of shallow shells with rectangular planform, varying thickness, and complicated boundary conditions.

1. Let us consider shallow shells with rectangular planform and thickness varying in two coordinate directions. We will use a refined formulation based on the hypothesis of rectilinear element. This hypothesis suggests that an element originally rectilinear and normal to the coordinate surface remains rectilinear after deformation but not normal, its length remaining the same.

According to this hypothesis, the displacements of a shell can be represented as

$$\begin{aligned}u_x(x, y, z) &= u(x, y) + z\psi_x(x, y), & u_y(x, y, z) &= v(x, y) + z\psi_y(x, y), \\u_z(x, y, z) &= w(x, y),\end{aligned}\tag{1}$$

---

S. P. Timoshenko Institute of Mechanics, National Academy of Sciences of Ukraine, Kyiv. Translated from *Prikladnaya Mekhanika*, Vol. 43, No. 10, pp. 80–91, October 2007. Original article submitted November 22, 2006.

where  $x$ ,  $y$ , and  $z$  are the coordinates of points of the shell;  $u_x$ ,  $u_y$ , and  $u_z$  are the respective displacements;  $u$ ,  $v$ , and  $w$  are the displacements of the coordinate surface along the  $x$ -,  $y$ -, and  $z$ -axes, respectively; and  $\psi_x$  and  $\psi_y$  are the complete angles of rotation of the rectilinear element.

According to (1), the strains are expressed as

$$\begin{aligned} e_x(x, y, z) &= \varepsilon_x(x, y) + z\kappa_x(x, y), & e_y(x, y, z) &= \varepsilon_y(x, y) + z\kappa_y(x, y), \\ e_{xy}(x, y, z) &= \varepsilon_{xy}(x, y) + z2\kappa_{xy}(x, y), & e_{xz}(x, y, z) &= \gamma_x(x, y), & e_{yz}(x, y, z) &= \gamma_y(x, y), \end{aligned} \quad (2)$$

where

$$\begin{aligned} \varepsilon_x &= \frac{\partial u}{\partial x} + k_1 w, & \varepsilon_y &= \frac{\partial v}{\partial y} + k_2 w, & \varepsilon_{xy} &= \frac{\partial u}{\partial y} + \frac{\partial v}{\partial x}, \\ \kappa_x &= \frac{\partial \psi_x}{\partial x} - k_1^2 w, & \kappa_y &= \frac{\partial \psi_y}{\partial y} - k_2^2 w, & 2\kappa_{xy} &= \frac{\partial \psi_x}{\partial y} + \frac{\partial \psi_y}{\partial x}, \\ \gamma_x &= \psi_x - \vartheta_x, & \gamma_y &= \psi_y - \vartheta_y, & \vartheta_x &= -\frac{\partial w}{\partial x} + k_1 u, & \vartheta_y &= -\frac{\partial w}{\partial y} + k_2 v, \end{aligned} \quad (3)$$

where  $\varepsilon_x$ ,  $\varepsilon_y$ , and  $\varepsilon_{xy}$  are the tangential strains of the coordinate surface;  $\kappa_x$ ,  $\kappa_y$ , and  $\kappa_{xy}$  are the flexural strains of the coordinate surface;  $k_1$  and  $k_2$  are the curvatures;  $\vartheta_x$  and  $\vartheta_y$  are the angles of rotation of the normal regardless of transverse shear; and  $\gamma_x$  and  $\gamma_y$  are the angles of rotation of the normal due to transverse shear. The equilibrium equations are

$$\begin{aligned} \frac{\partial N_x}{\partial x} + \frac{\partial N_{yx}}{\partial y} &= 0, & \frac{\partial N_y}{\partial y} + \frac{\partial N_{xy}}{\partial x} &= 0, & \frac{\partial Q_x}{\partial x} + \frac{\partial Q_y}{\partial y} - k_1 N_x - k_2 N_y + q &= 0, \\ \frac{\partial M_x}{\partial x} + \frac{\partial M_{yx}}{\partial y} - Q_x &= 0, & \frac{\partial M_y}{\partial y} + \frac{\partial M_{xy}}{\partial x} - Q_y &= 0, & N_{xy} - k_2 M_{yx} - N_{yx} - k_1 M_{xy} &= 0, \end{aligned} \quad (4)$$

where  $N_x$ ,  $N_y$ ,  $N_{xy}$ , and  $N_{yx}$  are the tangential forces;  $Q_x$  and  $Q_y$  are the shearing forces; and  $M_x$ ,  $M_y$ ,  $M_{xy}$ , and  $M_{yx}$  are the bending and twisting moments.

The elastic relations for orthotropic shells symmetric across the thickness about the chosen coordinate surface are

$$\begin{aligned} N_x &= C_{11}\varepsilon_x + C_{12}\varepsilon_y, & N_y &= C_{12}\varepsilon_x + C_{22}\varepsilon_y, \\ N_{xy} &= C_{66}\varepsilon_{xy} + 2k_2 D_{66}\kappa_{xy}, & N_{yx} &= C_{66}\varepsilon_{xy} + 2k_1 D_{66}\kappa_{xy}, \\ M_x &= D_{11}\kappa_x + D_{12}\kappa_y, & M_y &= D_{12}\kappa_x + D_{22}\kappa_y, \\ M_{yx} &= M_{xy} = 2D_{66}\kappa_{xy}, & Q_x &= K_1\gamma, & Q_y &= K_2\gamma_y, \end{aligned} \quad (5)$$

where

$$\begin{aligned} C_{11} &= \frac{E_x h}{1 - \nu_x \nu_y}, & C_{12} &= \nu_y C_{11}, & C_{22} &= \frac{E_y h}{1 - \nu_x \nu_y}, & C_{66} &= G_{xy} h, \\ D_{11} &= \frac{E_x h^3}{12(1 - \nu_x \nu_y)}, & D_{12} &= \nu_y D_{11}, & D_{22} &= \frac{E_y h^3}{12(1 - \nu_x \nu_y)}, & D_{66} &= \frac{G_{xy} h^3}{12}, \\ K_1 &= \frac{5}{6} h G_{xz}, & K_2 &= \frac{5}{6} h G_{yz}, \end{aligned} \quad (6)$$

where  $E_x$ ,  $E_y$  and  $\nu_x$ ,  $\nu_y$  are the elastic moduli and Poisson's ratios along the  $x$ - and  $y$ -axes;  $G_{xy}$ ,  $G_{xz}$ , and  $G_{yz}$  are the shear moduli; and  $h = h(x, y)$  is the thickness of the shell.

To determine the stresses in orthotropic shallow shells with rectangular planform, we will start with Hooke's law [1, 2, 4]:

$$\begin{aligned} e_x &= b_{11}\sigma_x + b_{12}\sigma_y, & e_y &= b_{12}\sigma_x + b_{22}\sigma_y, \\ e_{xy} &= b_{66}\tau_{xy}, & e_{xz} &= b_{55}\tau_{xz}, & e_{yz} &= b_{44}\tau_{yz}, \end{aligned} \quad (7)$$

where

$$\begin{aligned} b_{11} &= \frac{1}{E_x}, & b_{12} &= -\frac{\nu_x}{E_x} = -\frac{\nu_y}{E_y}, & b_{22} &= \frac{1}{E_y}, \\ b_{66} &= \frac{1}{G_{xy}}, & b_{44} &= \frac{1}{G_{yz}}, & b_{55} &= \frac{1}{G_{xz}}. \end{aligned} \quad (8)$$

Resolving Eqs. (7) for the stresses and using (2), we obtain an expression for stresses in terms of the strains of the coordinate surface:

$$\begin{aligned} (b_{11}b_{22} - b_{12}^2)\sigma_x &= b_{22}(\varepsilon_x + z\kappa_x) - b_{12}(\varepsilon_y + z\kappa_y), \\ (b_{12}^2 - b_{11}b_{22})\sigma_y &= b_{12}(\varepsilon_x + z\kappa_x) - b_{11}(\varepsilon_y + z\kappa_y), \\ b_{66}\tau_{xy} &= \varepsilon_{xy} + 2z\kappa_{xy}, & b_{55}\tau_{xz} &= \gamma_x, & b_{44}\tau_{yz} &= \gamma_y \quad \left(-\frac{h}{2} \leq z \leq \frac{h}{2}\right). \end{aligned} \quad (9)$$

If

$$\frac{\partial u}{\partial x} = \tilde{u}, \quad \frac{\partial v}{\partial x} = \tilde{v}, \quad \frac{\partial w}{\partial x} = \tilde{w}, \quad \frac{\partial \psi_x}{\partial x} = \tilde{\psi}_x, \quad \frac{\partial \psi_y}{\partial x} = \tilde{\psi}_y, \quad (10)$$

then the governing equations for the functions  $u, \tilde{u}, v, \tilde{v}, w, \tilde{w}, \psi_x, \tilde{\psi}_x, \psi_y, \tilde{\psi}_y$  are

$$\begin{aligned} \tilde{u} &= \frac{\partial u}{\partial x}, & \tilde{v} &= \frac{\partial v}{\partial x}, & \tilde{w} &= \frac{\partial w}{\partial x}, & \tilde{\psi}_x &= \frac{\partial \psi_x}{\partial x}, & \tilde{\psi}_y &= \frac{\partial \psi_y}{\partial x}, \\ \frac{\partial \tilde{u}}{\partial x} &= a_{11}\tilde{u} + a_{12}\frac{\partial \tilde{u}}{\partial y} + a_{13}\frac{\partial^2 \tilde{u}}{\partial y^2} + a_{14}\tilde{v} + a_{15}\frac{\partial \tilde{v}}{\partial y} + a_{16}\frac{\partial \tilde{v}}{\partial y} + a_{17}w + a_{18}\tilde{w} \\ &+ a_{19}\frac{\partial \tilde{\psi}_x}{\partial y} + a_{1,10}\frac{\partial^2 \tilde{\psi}_x}{\partial y^2} + a_{1,11}\tilde{\psi}_y + a_{1,12}\frac{\partial \tilde{\psi}_y}{\partial y}, \\ \frac{\partial \tilde{v}}{\partial x} &= a_{21}\tilde{u} + a_{22}\frac{\partial \tilde{u}}{\partial y} + a_{23}\frac{\partial \tilde{u}}{\partial y} + a_{24}v + a_{25}\tilde{v} + a_{26}\frac{\partial v}{\partial y} + a_{27}\frac{\partial^2 v}{\partial y^2} + a_{28}w \\ &+ a_{29}\frac{\partial w}{\partial y} + a_{2,10}\tilde{\psi}_x + a_{2,11}\frac{\partial \tilde{\psi}_x}{\partial y} + a_{2,12}\psi_y + a_{2,13}\frac{\partial \psi_y}{\partial y} + a_{2,14}\frac{\partial^2 \psi_y}{\partial y^2}, \\ \frac{\partial \tilde{w}}{\partial x} &= a_{31}u + a_{32}\tilde{u} + a_{33}v + a_{34}\frac{\partial v}{\partial y} + a_{35}w + a_{36}\tilde{w} + a_{37}\frac{\partial w}{\partial y} \\ &+ a_{38}\frac{\partial^2 w}{\partial y^2} + a_{39}\psi_x + a_{3,10}\tilde{\psi}_x + a_{3,11}\psi_y + a_{3,12}\frac{\partial \psi_y}{\partial y} + a_{3,13}q, \\ \frac{\partial \tilde{\psi}_x}{\partial x} &= a_{41}u + a_{42}w + a_{43}\tilde{w} + a_{44}\psi_x + a_{45}\tilde{\psi}_x + a_{46}\frac{\partial \psi_x}{\partial y} + a_{47}\frac{\partial^2 \psi_x}{\partial y^2} + a_{48}\tilde{\psi}_y + a_{49}\frac{\partial \psi_y}{\partial y} + a_{4,10}\frac{\partial \tilde{\psi}_y}{\partial y}, \end{aligned}$$

$$\frac{\partial \tilde{\Psi}_y}{\partial y} = a_{51}v + a_{52}w + a_{53} \frac{\partial w}{\partial y} + a_{54} \tilde{\Psi}_x + a_{55} \frac{\partial \Psi_x}{\partial y} + a_{56} \frac{\partial \Psi_x}{\partial y} + a_{57} \Psi_y + a_{58} \tilde{\Psi}_y + a_{59} \frac{\partial \Psi_y}{\partial y} + a_{5,10} \frac{\partial^2 \Psi_y}{\partial y^2}. \quad (11)$$

In the general case, the coefficients  $a_{ij}$  depend on  $x$  and  $y$ :

$$\begin{aligned} a_{11} &= -\frac{1}{C_{11}} \frac{\partial C_{11}}{\partial x}, & a_{12} &= -\frac{1}{C_{11}} \frac{\partial C_{66}}{\partial y}, & a_{13} &= -\frac{C_{66}}{C_{11}}, & a_{14} &= -\frac{1}{C_{11}} \frac{\partial C_{66}}{\partial y}, \\ a_{15} &= -\frac{1}{C_{11}} \frac{\partial C_{12}}{\partial x}, & a_{16} &= -\frac{C_{12} + C_{66}}{C_{11}}, & a_{17} &= -\frac{1}{C_{11}} \left( \frac{\partial C_{11}}{\partial x} k_1 + \frac{\partial C_{12}}{\partial x} k_2 \right), & a_{18} &= -\frac{C_{11} k_1 + C_{12} k_2}{C_{11}}, \\ a_{19} &= -\frac{k_1}{C_{11}} \frac{\partial D_{66}}{\partial y}, & a_{1,10} &= -\frac{k_1 D_{66}}{C_{11}}, & a_{1,11} &= -\frac{k_1}{C_{11}} \frac{\partial D_{66}}{\partial y}, & a_{1,12} &= -\frac{k_1 D_{66}}{C_{11}}, \\ a_{21} &= -\frac{1}{C_{66}} \frac{\partial C_{12}}{\partial y}, & a_{22} &= -\frac{1}{C_{66}} \frac{\partial C_{66}}{\partial x}, & a_{23} &= -\frac{C_{12} + C_{66}}{C_{66}}, \\ a_{24} &= \frac{K_2 k_2^2}{C_{66}}, & a_{25} &= -\frac{1}{C_{66}} \frac{\partial C_{66}}{\partial x}, & a_{26} &= -\frac{1}{C_{66}} \frac{\partial C_{22}}{\partial y}, & a_{27} &= -\frac{C_{22}}{C_{66}}, \\ a_{28} &= -\left( \frac{k_1^2 k_2}{C_{66}} \frac{\partial D_{22}}{\partial y} + \frac{k_2^3}{C_{66}} \frac{\partial D_{22}}{\partial y} + \frac{1}{C_{66}} \left( \frac{\partial C_{12}}{\partial y} k_1 + \frac{\partial C_{22}}{\partial y} k_2 \right) \right), \\ a_{29} &= -\left( \frac{k_1^2 k_2 D_{12}}{C_{66}} + \frac{k_2^3 D_{22}}{C_{66}} + \frac{K_2 k_2}{C_{66}} + \frac{C_{12} k_1 + C_{22} k_2}{C_{66}} \right), & a_{2,10} &= \frac{k_2}{C_{66}} \frac{\partial D_{12}}{\partial y}, \\ a_{2,11} &= \frac{k_2 D_{12}}{C_{66}}, & a_{2,12} &= -\frac{K_2 k_2}{C_{66}}, & a_{2,13} &= \frac{k_2}{C_{66}} \frac{\partial D_{22}}{\partial y}, & a_{2,14} &= \frac{k_2 D_{22}}{C_{66}}, \\ a_{31} &= \frac{k_1}{K_1} \frac{\partial K_1}{\partial x}, & a_{32} &= k_1 + \frac{k_1 C_{11}}{K_1} + \frac{k_2 C_{12}}{K_1}, & a_{33} &= \frac{k_2}{K_1} \frac{\partial K_2}{\partial y}, \\ a_{34} &= \frac{K_2 k_2}{K_1} + \frac{k_1 C_{12}}{K_1} + \frac{k_2 C_{22}}{K_1}, & a_{35} &= \frac{k_1^2 C_{11}}{K_1} + 2 \frac{k_1 k_2 C_{12}}{K_1} + \frac{k_2^2 C_{22}}{K_1}, \\ a_{36} &= -\frac{1}{K_1} \frac{\partial K_1}{\partial x}, & a_{37} &= -\frac{1}{K_1} \frac{\partial K_2}{\partial y}, & a_{38} &= -\frac{K_2}{K_1}, & a_{39} &= -\frac{1}{K_1} \frac{\partial K_1}{\partial x}, \\ a_{3,10} &= -1, & a_{3,11} &= -\frac{1}{K_1} \frac{\partial K_2}{\partial y}, & a_{3,12} &= -\frac{K_2}{K_1}, & a_{3,13} &= -\frac{1}{K_1}, \\ a_{41} &= -\frac{K_1 k_1}{D_{11}}, & a_{42} &= \frac{k_1^2}{D_{11}} \frac{\partial D_{11}}{\partial x} + \frac{k_2^2}{D_{11}} \frac{\partial D_{12}}{\partial x}, & a_{43} &= k_1^2 + \frac{D_{12} k_2^2}{D_{11}} + \frac{K_1}{D_{11}}, & a_{44} &= \frac{K_1}{D_{11}}, \\ a_{45} &= -\frac{1}{D_{11}} \frac{\partial D_{11}}{\partial x}, & a_{46} &= -\frac{1}{D_{11}} \frac{\partial D_{66}}{\partial y}, & a_{47} &= -\frac{D_{66}}{D_{11}}, & a_{48} &= -\frac{1}{D_{11}} \frac{\partial D_{66}}{\partial y}, \\ a_{49} &= -\frac{1}{D_{11}} \frac{\partial D_{12}}{\partial x}, & a_{4,10} &= -\left( \frac{D_{12}}{D_{11}} + \frac{D_{66}}{D_{11}} \right), & a_{51} &= -\frac{K_2 k_2}{D_{66}}, & a_{52} &= \frac{k_1^2}{D_{66}} \frac{\partial D_{12}}{\partial y} + \frac{k_2^2}{D_{66}} \frac{\partial D_{22}}{\partial y}, \end{aligned}$$

$$a_{53} = \frac{D_{12}}{D_{66}} k_1^2 + \frac{D_{22}}{D_{66}} k_2^2 + \frac{K_2}{D_{66}}, \quad a_{54} = -\frac{1}{D_{66}} \frac{\partial D_{12}}{\partial y}, \quad a_{55} = -\frac{1}{D_{66}} \frac{\partial D_{66}}{\partial x}, \quad a_{56} = -\left(\frac{D_{12}}{D_{66}} + 1\right),$$

$$a_{57} = \frac{K_2}{D_{66}}, \quad a_{58} = -\frac{1}{D_{66}} \frac{\partial D_{66}}{\partial x}, \quad a_{59} = -\frac{1}{D_{66}} \frac{\partial D_{22}}{\partial y}, \quad a_{5,10} = -\frac{D_{22}}{D_{66}}. \quad (12)$$

We will consider the following boundary conditions:

(i) all edges are clamped:

$$u = v = w = \psi_x = \psi_y = 0 \quad \text{at} \quad x = 0, \quad x = a, \quad y = 0, \quad y = b, \quad (13)$$

(ii) three edges are clamped and one edge is hinged:

$$u = v = w = \psi_x = \psi_y = 0 \quad \text{at} \quad x = 0, \quad y = 0, \quad y = b,$$

$$\frac{\partial u}{\partial x} = v = w = \frac{\partial \psi_x}{\partial x} = \psi_y = 0 \quad \text{at} \quad x = a, \quad (14)$$

(iii) two edges are clamped and two edges are hinged:

$$u = v = w = \psi_x = \psi_y = 0 \quad \text{at} \quad y = 0, \quad y = b,$$

$$\frac{\partial u}{\partial x} = v = w = \frac{\partial \psi_x}{\partial x} = \psi_y = 0 \quad \text{at} \quad x = 0, \quad x = a. \quad (15)$$

2. To solve two-dimensional boundary-value problems of the class under consideration, the desired solution is approximated by spline functions in one coordinate direction, and the resulting one-dimensional boundary-value problem is solved by the stable discrete-orthogonalization method [2, 13–16].

The system of equations (11) includes no higher than second-order derivatives of unknown functions with respect to the coordinate  $y$ . Therefore, it is sufficient to use cubic spline functions to approximate solutions in  $y$ . Then the solution of the boundary-value problem for the system of equations (11) with appropriate boundary conditions can be represented in the following form [13–17]:

$$u(x, y) = \sum_{i=0}^N u_i(x) \varphi_{1i}(y), \quad v(x, y) = \sum_{i=0}^N v_i(x) \varphi_{2i}(y), \quad w(x, y) = \sum_{i=0}^N w_i(x) \varphi_{3i}(y),$$

$$\psi_x(x, y) = \sum_{i=0}^N \psi_\xi(x) \varphi_{4i}(y), \quad \psi_y(x, y) = \sum_{i=0}^N \psi_{y_i}(x) \varphi_{5i}(y), \quad (16)$$

where  $u_i(x), v_i(x), w_i(x), \psi_\xi(x)$ , and  $\psi_{y_i}(x)$  are the required functions of the variable  $x$ ;  $\varphi_{ji}(y)$  ( $j = \overline{1,5}$ ) are linear combinations of B-splines on a uniform mesh  $\Delta: 0 = y_0 < y_1 < \dots < y_N = b$ , satisfying the boundary conditions on  $y = 0$  and  $y = b$ . The system includes no higher than second-order derivatives of unknown functions with respect to the coordinate  $y$ ; therefore, it is sufficient to use cubic splines:

$$B_3^i(y) = \begin{cases} 0, & -\infty < y < y_{i-2}, \\ z^3, & y_{i-2} \leq y < y_{i-1}, \\ -3z^3 + 3z^2 + 3z + 1, & y_{i-1} \leq y < y_i, \\ 3z^3 - 6z^2 + 4, & y_i \leq y < y_{i+1}, \\ (1-z)^3, & y_{i+1} \leq y < y_{i+2}, \\ 0, & y_{i+2} \leq y < \infty, \end{cases} \quad (17)$$

where  $z = (y - y_k)/h_y$ , on the interval  $[y_k, y_{k+1}]$ ,  $k = \overline{i-2, i+1}$ ,  $i = \overline{-1, N+1}$ ,  $h_y = y_{k+1} - y_k = \text{const}$ .

The functions  $\varphi_{ji}(y)$  are set up as follows:

(i) if an unknown function is equal to zero, then

$$\begin{aligned}\varphi_{j0}(y) &= -4B_3^{-1}(y) + B_3^0(y), & \varphi_{j1}(y) &= B_3^{-1}(y) - \frac{1}{2}B_3^0(y) + B_3^1(y), \\ \varphi_{ji}(y) &= B_3^i(y) \quad (i = 2, 3, \dots, N-2);\end{aligned}\tag{18}$$

(ii) if the derivative of an unknown function with respect to  $y$  is equal to zero, then

$$\begin{aligned}\varphi_{j0}(y) &= B_3^0(y), & \varphi_{j1}(y) &= B_3^{-1}(y) - \frac{1}{2}B_3^0(y) + B_3^1(y), \\ \varphi_{ji}(y) &= B_3^i(y) \quad (i = 2, 3, \dots, N-2).\end{aligned}\tag{19}$$

The functions  $\varphi_{j,N-1}(y)$  and  $\varphi_{j,N}(y)$  are represented similarly.

Substituting solution (16) into the governing system of equations (11) and requiring them to be satisfied at set collocation points  $\xi_k \in [0, b]$ ,  $k = \overline{0, N}$ , we obtain a system of ordinary differential equations of the  $10(N+1)$ th order for the functions  $u_i, \tilde{u}_i, v_i, \tilde{v}_i, w_i, \tilde{w}_i, \Psi_\xi, \tilde{\Psi}_\xi, \Psi_{y_i},$  and  $\tilde{\Psi}_{y_i}$  ( $i = 0, \dots, N$ ). If

$$\Phi_{j\alpha} = [\varphi_{ji}^{(\alpha)}(\xi_k)]: \quad (i, k = \overline{0, N}), \quad j = 1, \dots, 5, \quad \alpha = 0, 1, 2$$

$$\bar{u} = [u_0, u_1, \dots, u_N]^T, \quad \bar{v} = [v_0, v_1, \dots, v_N]^T, \quad \bar{w} = [w_0, w_1, \dots, w_N]^T,$$

$$\bar{\Psi}_x = [\Psi_{x0}, \Psi_{x1}, \dots, \Psi_{xN}]^T, \quad \bar{\Psi}_y = [\Psi_{y0}, \Psi_{y1}, \dots, \Psi_{yN}]^T, \quad \bar{q} = [q(x, \xi_0), q(x, \xi_1), \dots, q(x, \xi_N)]^T$$

and if  $A = [a_{ij}]$  ( $i, j = \overline{0, N}$ ) and  $\bar{c} = [c_0, c_1, \dots, c_N]^T$ , then  $\bar{c} * A$  denotes the matrix  $[c_i a_{ij}]$ . Also, if  $\bar{d} = [d_0, d_1, \dots, d_N]^T$ , then  $\bar{c} * \bar{d} = [c_0 d_0, c_1 d_1, \dots, c_N d_N]^T$ .

Now the system of ordinary differential equations for  $u, \tilde{u}, v, \tilde{v}, w, \tilde{w}, \Psi_x, \tilde{\Psi}_x, \Psi_y,$  and  $\tilde{\Psi}_y$  becomes

$$\begin{aligned}\frac{d\bar{u}}{dx} &= \Phi_{10}^{-1}(\bar{a}_{12} * \Phi_{11} + \bar{a}_{13} * \Phi_{12})\bar{u} + \Phi_{10}^{-1}(\bar{a}_{11} * \Phi_{10})\bar{u}' + \Phi_{10}^{-1}(\bar{a}_{15} * \Phi_{21})\bar{v} + \Phi_{10}^{-1}(\bar{a}_{14} * \Phi_{20} \\ &\quad + \bar{a}_{16} * \Phi_{21})\bar{v}' + \Phi_{10}^{-1}(\bar{a}_{17} * \Phi_{30})\bar{w} + \Phi_{10}^{-1}(\bar{a}_{18} * \Phi_{30})\bar{w}' \\ &\quad + \Phi_{10}^{-1}(\bar{a}_{19} * \Phi_{41} + \bar{a}_{1,10} * \Phi_{42})\bar{\Psi}_x + \Phi_{10}^{-1}(\bar{a}_{1,11} * \Phi_{50} + \bar{a}_{1,12} * \Phi_{51})\bar{\Psi}_y', \\ \frac{d\bar{v}}{dx} &= \Phi_{20}^{-1}(\bar{a}_{22} * \Phi_{11})\bar{u} + \Phi_{20}^{-1}(\bar{a}_{21} * \Phi_{10} + \bar{a}_{23} * \Phi_{11})\bar{u}' \\ &\quad + \Phi_{20}^{-1}(\bar{a}_{24} * \Phi_{20} + \bar{a}_{26} * \Phi_{21} + \bar{a}_{27} * \Phi_{22})\bar{v} + \Phi_{20}^{-1}(\bar{a}_{25} * \Phi_{20})\bar{v}' \\ &\quad + \Phi_{20}^{-1}(\bar{a}_{28} * \Phi_{30} + \bar{a}_{29} * \Phi_{31})\bar{w} + \Phi_{20}^{-1}(\bar{a}_{2,10} * \Phi_{40} + \bar{a}_{2,11} * \Phi_{41})\bar{\Psi}_x' \\ &\quad + \Phi_{20}^{-1}(\bar{a}_{2,12} * \Phi_{50} + \bar{a}_{2,13} * \Phi_{51} + \bar{a}_{2,14} * \Phi_{52})\bar{\Psi}_y, \\ \frac{d\bar{w}}{dx} &= \Phi_{30}^{-1}(\bar{a}_{31} * \Phi_{10})\bar{u} + \Phi_{30}^{-1}(\bar{a}_{32} * \Phi_{10})\bar{u}' + \Phi_{30}^{-1}(\bar{a}_{33} * \Phi_{20} + \bar{a}_{34} * \Phi_{21})\bar{v} \\ &\quad + \Phi_{30}^{-1}(\bar{a}_{35} * \Phi_{30} + \bar{a}_{37} * \Phi_{31} + \bar{a}_{38} * \Phi_{32})\bar{w} + \Phi_{30}^{-1}(\bar{a}_{36} * \Phi_{30})\bar{w}' \\ &\quad + \Phi_{30}^{-1}(\bar{a}_{39} * \Phi_{40})\bar{\Psi}_x + \Phi_{30}^{-1}(\bar{a}_{3,10} * \Phi_{40})\bar{\Psi}_x' + \Phi_{30}^{-1}(\bar{a}_{3,11} * \Phi_{50} + \bar{a}_{3,12} * \Phi_{51})\bar{\Psi}_y + \Phi_{30}^{-1}(\bar{a}_{3,13} * q),\end{aligned}$$

TABLE 1

$x/a$	Spline-approximation method				Analytic solution
	$N=9$	$N=13$	$N=17$	$N=21$	
0.1	1098.8	1112.7	1117.3	1119.3	1121.0
0.2	2016.7	2043.9	2052.9	2056.6	2060.0
0.3	2679	2717.4	2730	2735.4	2740.0
0.4	3070.9	3117	3132.3	3138.6	3144.3
0.5	3199.8	3248.8	3264.9	3271.7	3277.7

$$\begin{aligned}
 \frac{d\bar{\psi}_x}{dx} &= \Phi_{40}^{-1}(\bar{a}_{41} * \Phi_{10})\bar{u} + \Phi_{40}^{-1}(\bar{a}_{42} * \Phi_{30})\bar{w} + \Phi_{40}^{-1}(\bar{a}_{43} * \Phi_{30})\bar{w}' \\
 &+ \Phi_{40}^{-1}(\bar{a}_{44} * \Phi_{40} + \bar{a}_{46} * \Phi_{41} + \bar{a}_{47} * \Phi_{42})\bar{\psi}_x + \Phi_{40}^{-1}(\bar{a}_{45} * \Phi_{40})\bar{\psi}'_x \\
 &+ \Phi_{40}^{-1}(\bar{a}_{49} * \Phi_{51})\bar{\psi}_y + \Phi_{40}^{-1}(\bar{a}_{48} * \Phi_{50} + \bar{a}_{4,10} * \Phi_{51})\bar{\psi}'_y, \\
 \frac{d\bar{\psi}_y}{dx} &= \Phi_{50}^{-1}(\bar{a}_{51} * \Phi_{20})\bar{v} + \Phi_{50}^{-1}(\bar{a}_{52} * \Phi_{30} + \bar{a}_{53} * \Phi_{31})\bar{w} + \Phi_{50}^{-1}(\bar{a}_{55} * \Phi_{41})\bar{\psi}_x + \Phi_{50}^{-1}(\bar{a}_{54} * \Phi_{40} \\
 &+ \bar{a}_{56} * \Phi_{41})\bar{\psi}'_x + \Phi_{50}^{-1}(\bar{a}_{57} * \Phi_{50} + \bar{a}_{59} * \Phi_{51} + \bar{a}_{5,10} * \Phi_{52})\bar{\psi}_y + \Phi_{50}^{-1}(\bar{a}_{58} * \Phi_{50})\bar{\psi}'_y,
 \end{aligned} \tag{20}$$

which can be represented as

$$\frac{d\bar{Y}}{dx} = A\bar{Y} + \bar{f}, \tag{21}$$

where

$$\begin{aligned}
 \bar{Y} &= \{u_0, \dots, u_N, \tilde{u}_0, \dots, \tilde{u}_N, v_0, \dots, v_N, \tilde{v}_0, \dots, \tilde{v}_N, w_0, \dots, w_N, \tilde{w}_0, \dots, \tilde{w}_N, \\
 &\Psi_{x0}, \dots, \Psi_{xN}, \tilde{\Psi}_{x0}, \dots, \tilde{\Psi}_{xN}, \Psi_{y0}, \dots, \Psi_{yN}, \tilde{\Psi}_{y0}, \dots, \tilde{\Psi}_{yN}\}^T
 \end{aligned}$$

is a vector function of  $x$ ;  $\bar{f}$  is the vector of right-hand sides;  $A$  is a square matrix whose elements depend on  $x$ .

The boundary conditions for this system read

$$B_1\bar{Y}(x_1) = \bar{b}_1, \quad B_2\bar{Y}(x_2) = \bar{b}_2. \tag{22}$$

The one-dimensional boundary-value problem (21), (22) is solved by the stable discrete-orthogonalization method.

To estimate the accuracy of our method, we will compare the stress states of an isotropic shallow shell with square planform, constant thickness, and hinged edges obtained by the spline-collocation method followed by the discrete-orthogonalization method and by the method of double trigonometric series using the expansion

$$u = \sum_{m=1,3,\dots}^{\infty} \sum_{n=1,3,\dots}^{\infty} a_{mn} \cos \frac{m\pi x}{a} \sin \frac{n\pi y}{b}, \quad v = \sum_{m=1,3,\dots}^{\infty} \sum_{n=1,3,\dots}^{\infty} b_{mn} \sin \frac{m\pi x}{a} \cos \frac{n\pi y}{b},$$

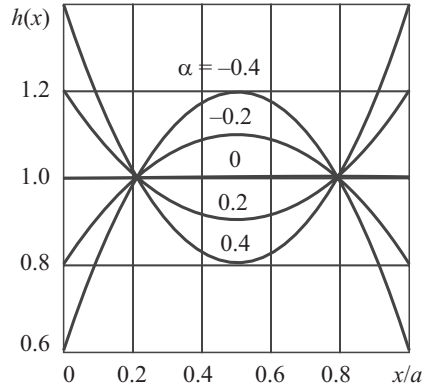


Fig. 1

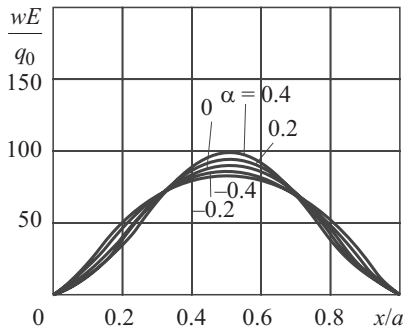


Fig. 2

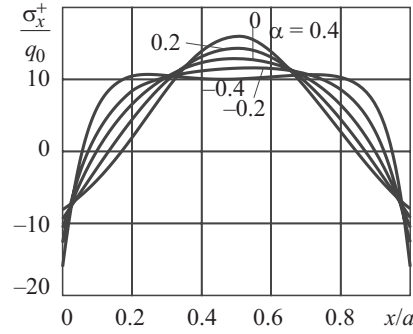


Fig. 3

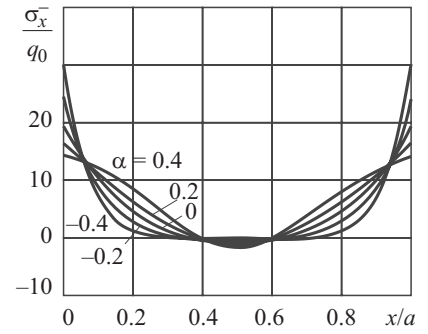


Fig. 4

$$w = \sum_{m=1,3,\dots}^{\infty} \sum_{n=1,3,\dots}^{\infty} c_{mn} \sin \frac{m\pi x}{a} \sin \frac{n\pi y}{b},$$

$$\psi_x = \sum_{m=1,3,\dots}^{\infty} \sum_{n=1,3,\dots}^{\infty} d_{mn} \cos \frac{m\pi x}{a} \sin \frac{n\pi y}{b}, \quad \psi_y = \sum_{m=1,3,\dots}^{\infty} \sum_{n=1,3,\dots}^{\infty} e_{mn} \sin \frac{m\pi x}{a} \cos \frac{n\pi y}{b}. \quad (23)$$

Table 1 presents the results (values of the deflection  $wE/q_0$  at some points of the mid-surface for  $y = a/2$ ) of stress-strain analysis of the shell under a distributed load  $q = q_0 = \text{const}$  obtained by the spline-collocation method with different number of collocation points and from the analytic solution (23). The shell is characterized by the following parameters:  $a = 10$ ,  $h = 0.4$ ,  $k_1 = 0.05$ ,  $k_2 = 0$ ,  $\nu = 0.3$ . It can be seen that as the number of collocation points increases, the numerical results closely approach the analytic solution, which may serve as a reliability criterion for our method.

**3.** Let us analyze, as an example, the stress-strain state a doubly curved isotropic shallow shell with square platform and varying thickness under uniform normal pressure  $q = q_0 = \text{const}$ .

We will examine three types of boundary conditions: (13), (14), and (15). The thickness of the shell (Fig. 1) varies as

$$h(x) = \left[ \alpha \left( 6 \frac{x^2}{a^2} - 6 \frac{x}{a} + 1 \right) + 1 \right] h_0, \quad (24)$$

where  $h_0 = \text{const}$ .

With such variation in the thickness, the weight of the shell remains constant. The input data:  $a = b = 10$ ,  $k_1 = 1/10$ ,  $k_2 = 0$ ,  $\alpha = -0.4, -0.2, 0, 0.2, 0.4$ ,  $\nu = 0.3$ ,  $h_0 = 1$ .



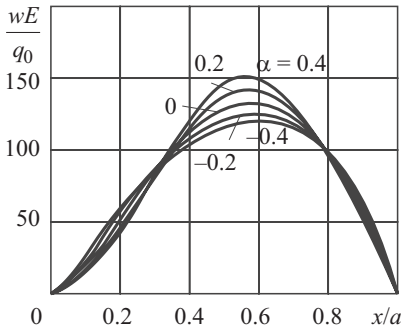


Fig. 5

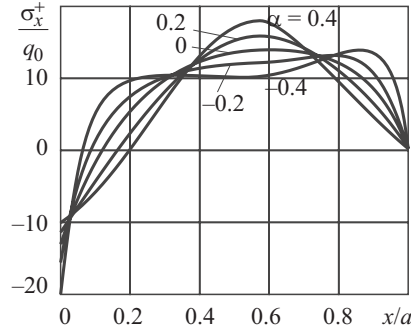


Fig. 6

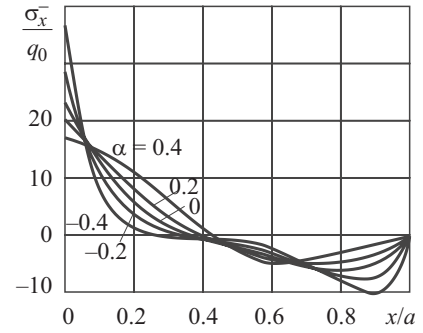


Fig. 7

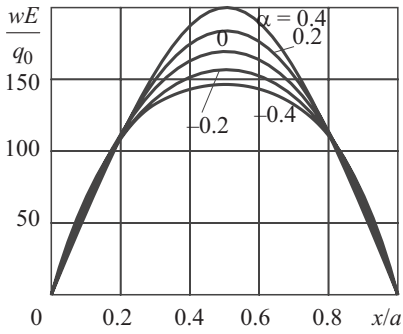


Fig. 8

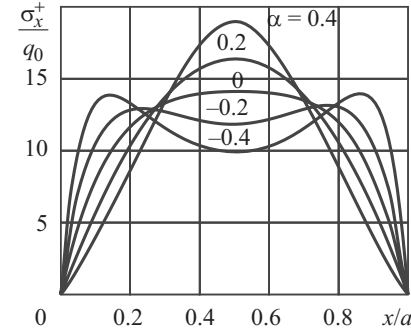


Fig. 9

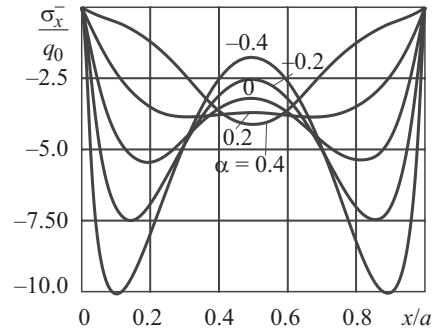


Fig. 10

Figure 1 demonstrates the behavior of the thickness  $h(x)$ . The values of  $h(x)$  are symmetrically distributed about the rise in the mid-section.

Figures 2–4 show the thickness dependence of the deflection and stresses in the section  $y = a/2$  on the lateral surfaces of the shell clamped at all edges. As is seen,  $w$ ,  $\sigma_x^+$ , and  $\sigma_x^-$  are symmetrically distributed about the rise in the mid-section. It follows from Fig. 2 that the deflection peaks at the point of the rise, the maximum increasing with  $\alpha$ . As the thickness increases in this zone, its value decreases insignificantly. Figure 3 shows the stresses on the outside surface as a function of the thickness. It can be seen that  $\sigma_x^+$  peaks at the point of the rise, the maximum increasing with  $\alpha$ . Figure 4 shows the stress distribution on the inside surface of the shell. The stress patterns on the inside and outside surfaces are qualitatively close and differ by sign. Quantitatively, the maximum stresses  $\sigma_x^-$  are almost twice as great as  $\sigma_x^+$ .

Figures 5–7 show the thickness dependence of the deflection and stresses in the section  $y = a/2$  on the lateral surfaces of the shell clamped at three edges and hinged at one edge. It can be seen that  $w$ ,  $\sigma_x^+$ , and  $\sigma_x^-$  are distributed asymmetrically. Figure 5 demonstrates that the maximum deflection is slightly shifted from the point of the rise toward the hinged edge, the maximum increasing with  $\alpha$ . As the thickness increases in this zone, the deflection decreases insignificantly. Figure 6 shows how the stress on the outside surface depends on the thickness. It can be seen that the maximum of  $\sigma_x^+$  is shifted from the point of the rise toward the hinged edge and increases with  $\alpha$ . Figure 7 shows the stress distribution on the inside surface. The stress patterns on the inside and outside surfaces of the shell are qualitatively close and differ by sign. Quantitatively, the maximum stresses  $\sigma_x^-$  are almost twice as great as  $\sigma_x^+$ .

Figures 8–10 show the thickness dependence of the deflection and stresses in the section  $y = a/2$  on the lateral surfaces of the shell with two opposite edges clamped and the other two edges hinged. It can be seen that  $w$ ,  $\sigma_x^+$ , and  $\sigma_x^-$  are distributed symmetrically about the rise in the mid-section. It follows from Fig. 8 that the deflection peaks at the point of the rise, the maximum increasing with  $\alpha$ . As the thickness decreases in this zone, the deflection increases insignificantly. Figure 9 demonstrates how the stress on the outside surface of the shell depends on the thickness. It can be seen that the maximum of  $\sigma_x^+$  is

at the point of the rise and increases with  $\alpha$ . Figure 10 shows the stress distribution on the inside surface of the shell. The stress patterns on the inside and outside surfaces are qualitatively close and differ by sign. Quantitatively, the maximum stresses  $\sigma_x^+$  are almost twice as great as  $\sigma_x^-$ .

Thus, by varying the thickness of a shell, it is possible to change the distribution of displacements and stresses, keeping its weight constant. The method outlined here can also be used to analyze the stress–strain state of shallow shells with rectangular planform and variable thickness in the anisotropic case.

## REFERENCES

1. V. Z. Vlasov, *General Theory of Shells* [in Russian], Gl. Izd. Tekhn.-Teor. Lit., Moscow–Leningrad (1949).
2. Ya. M. Grigorenko and A. T. Vasilenko, *Theory of Shells of Variable Stiffness* [in Russian], Naukova Dumka, Kyiv (1981).
3. Ya. M. Grigorenko, Yu. N. Shevchenko, A. T. Vasilenko, et al., *Numerical Methods* [in Russian], A.S.K., Kyiv (2002).
4. A. A. Nazarov, *Fundamentals of the Theory and Methods of Design of Shallow Shells* [in Russian], Stroiizdat, Leningrad (1966).
5. B. L. Pelekh, *Theory of Shells with Finite Shear Stiffness* [in Russian], Naukova Dumka, Kyiv (1973).
6. P. M. Varvak and A. F. Ryabov (eds.), *A Handbook of the Theory of Elasticity* [in Russian], Budivel'nyk, Kyiv (1971).
7. C. R. Calladine, *Theory of Shell Structures*, Cambridge Univ. Press, Cambridge (1983).
8. Y. K. Cheung, *Finite Strip Method in Structure Analysis*, Pergamon Press, Oxford (1976).
9. G. R. Cowper, G. M. Lindberg, and M. D. Olson, "Shallow shell finite element of triangular shape," *Int. J. Solids Struct.*, No. 6, 1133–1156 (1970).
10. S. C. Fan and Y. K. Cheung, "Analysis of shallow shells by spline finite strip method," *Eng. Struct.*, No. 5, 255–263 (1983).
11. W. Flügge, *Stresses in Shells*, Springer-Verlag, Berlin (1973).
12. P. L. Gould, *Analysis of Shells and Plates*, Springer-Verlag, New York (1988).
13. A. Ya. Grigorenko and T. L. Efimova, "Application of spline-approximation for solving the problems on natural vibrations of rectangular plates of variable thickness," *Int. Appl. Mech.*, **41**, No. 10, 1161–1169 (2005).
14. Ya. M. Grigorenko, A. Ya. Grigorenko, and L. I. Zakhariichenko, "Calculation of stress–strain state of orthotropic closed and open non-circular cylindrical shells," *Int. Appl. Mech.*, **41**, No. 7, 778–785 (2005).
15. Ya. M. Grigorenko, N. N. Kryukov, and N. S. Yakovenko, "Solving the boundary problems of the theory of layered orthotropic trapezoidal plates of variable thickness on the base of spline-approximation," *Int. Appl. Mech.*, **41**, No. 4, 413–420 (2005).
16. Ya. M. Grigorenko and S. N. Yaremchenko, "Refined design of corrugated noncircular cylindrical shells," *Int. Appl. Mech.*, **41**, No. 1, 7–13 (2005).
17. Ya. M. Grigorenko and L. I. Zakhariichenko, "Study into the effect of circumferential variation in thickness and load on the deformation," *Int. Appl. Mech.*, **38**, No. 10, 1229–1236 (2002).
18. E. Reissner, "Effect of transverse shear deformation on the bending of elastic plates," *Trans. ASME, J. Appl. Mech.*, No. 12, 69–77 (1945).
19. Z. Rychter, "Family of shear deformation theories for shallow shells," *Adv. Mech.*, No. 98, 221–232 (1993).